Iris localization using Daugman's algorithm

Oad Percy
Ahmad Waqas

This thesis is presented as part of degree of
Bachelor's of Science in Electrical Engineering

Blekinge Institute of Technology

Blekinge Institute of Technology
School of Engineering
Supervisor: Irina Gertsovich
Examiner: Dr. Sven Johansson

Abstract

Iris recognition system is a reliable and an accurate biometric system. Localization of the iris borders in an eye image can be considered as a vital step in the iris recognition process. There exist many algorithms to segment the iris. One of the segmentation methods, that is used in many commercial iris biometric systems is an algorithm known as a Daugman's algorithm. The aim of this thesis is to implement this algorithm using MATLAB programming environment. The implemented algorithm was tested on the eye images of different quality, such as the images with partly covered iris or low contrast images. The test results demonstrated that the Daugman's algorithm detects the iris borders in the high quality images with high accuracy. The performance of the algorithm on the lower quality images has been improved by additional preprocessing of these images.

Acknowledgement

We would like to express our sincere acknowledgement to our supervisor Ms. Irina Gertsovich. This thesis project would not have been possible without her encouragement and support.

Contents:

1 Introduction 13

1.1 Biometric in general 13

1.2 Iris biometric 13

1.3 Iris compared to other biometrics 14

1.4 Overview of methods to segment iris 14

2 Daugman's algorithm description 15

2.1 Daugman's operator: 15

2.2 Two dimensional 2D Gaussian filter 15

2.3 Two dimensional 2D convolution 16

2.4 The Daugman's operator explained 17

3 The enhancement of an eye image before the application of the Daugman's operator 19

3.1 Countering the effect of light reflection on images 19

3.2 Thresholding 21

3.3 Detecting pixels with locally minimal intensity values (local minima pixels) 21

3.4 No circles outside the image 21

3.5 Result 22

4 Plotting the results of the performance of the Daugman's operator 25

4.1 Graph of sum of circumferential pixels intensity values for the detected iris border 25

4.2 Graph of sum of circumferential pixels intensity values for a pixel near the detected iris outer border.. 26

5 Effect of the covering of the part of an eye image by an eyelid on the Daugman's operator performance 27

5.1 Daugman's suggestion to solve 'occlusion by eyelid' problem 28

5.2 Results obtained by using Daugman's suggestion to solve 'occlusions by eyelid' problem 30

5.3 Failure to solve 'occlusion by eyelid' problem using the Daugman's suggestion 31

6 Pupil detection (iris-pupil radii relation) 33

6.1 Results for pupil and iris detection 34

7 Image enhancement techniques 37

7.1 Histogram equalization 37
7.2 Contrast enhancement 39
8 Effect of image noise on Daugman's integrodifferential operator performance 43
9 Appendix A 45
9.1 Flow chart describing Daugman's method 45
10 References 47

List of Figures

Figure 1-1: Image of an eye representing the iris, pupil and sclera. 13
Figure 2-1: Graph of the 1D Gaussian filter as used in the thesis. 16
Figure 2-2: The black boxed line represents one pixel wide iris border at a certain radius 'R' (not to scale) at the centre coordinate and the blue boxed line represents one pixel wide circle at the same center coordinate at radius 'R+1'. 17
Figure 2-3: Two white circles representing two contours that are 1 pixel radius apart representing the concept of 'adjacent radii circles'. 18
Figure 3-1: (a) Light reflection affected eye image of size 164 by 246 pixels (b) Light reflection affected eye image of size 178 by 238 pixels. 19
Figure 3-2: (a) Iris and pupil wrongly detected for light reflection affected image for the input image shown in Figure 3-1(a) (b) Iris and pupil wrongly detected for light reflection affected image as shown in Figure-3-1(b). 20
Figure 3-3: (a) Output for the input image as shown in Figure 3-1(a) after the morphological operation (b) Output for the input image as shown in Figure 3-1(b) after applying the morphological operation. 20
Figure 3-4: Image showing the different circular contours at a range of radii. 22
Figure 3-5: Image showing object pixels after thresholding and local minima pixel detection. 22
Figure 3-6: Output image that shows limbic border of the iris (the white circle). 23
Figure 4-1: Image of the eye indicating the calculated centre pixel with coordinates (X, Y) = (127, 85) 25
Figure 4-2: Graph shows the dependence of the sum of circumferential pixel intensity values versus radius for a center pixel, shown in Figure 4-1. 25
Figure 4-3: Image of the eye indicating a pixel near the centre pixel with coordinates (X, Y) = (129, 84) 26
Figure 4-4: Graph at the pixel in figure 4-3 (a pixel near the centre of the iris), of the change in sum of circumferential pixel intensity values against increase in radius. 26
Figure 5-1: image with upper part of the iris covered by the eyelid. 27
Figure 5-2: Iris wrongly detected using Daugman's operator on the image with upper part of the iris covered by the eyelid as shown in Figure 5-1. 27
Figure 5-3: 50% (25% lateral left and 25% lateral right) of the circumference at the specified angles, to be used for iris border estimations, shown by the green arcs. 28
Figure 5-4: Daugman's assumption to use the proposed 50 % circumference. The green and blue arcs represent the iris border at radius 'R' and 'R+1'. 29
Figure 5-5: At every object pixel denoted by 'X' (not all object pixels shown), calculations at increasing radius, at every two adjacent radii (i.e. R & R+1) as shown by the red and brown circles, only the pixels in green arc are subtracted by the pixels in blue arc for calculations. 29
Figure 5-6: Iris outer border correctly determined in 'iris covered by eyelid' image using 50% circumference 30
Figure 5-7: Iris outer border detected in 'iris covered by eyelid' image of size 153 by 228 pixels using 50% circumference. 30
Figure 5-8: Iris outer border detected in 'iris covered by eyelid' image of size 126 by 198 pixels using 50% circumference. 31

Figure 5-9: (a) Eyelid covered image of size 171 by 294 pixels with the eyeball moved to an angle such that most of the upper, the lateral left portion and most of the lower part the iris border are covered by the eyelid (b) Iris incorrectly determined using 50% circumference approach. 31
Figure 5-10: Image representing the tilted angle showing that only 3/8th of the iris border is visible since the eyeball has a shift to the left. 32
Figure 6-1: Daugman's suggestion about the relationship between the radii of the iris border with the sclera and the iris border with the pupil. 33
Figure 6-2: Daugman's suggestion about the relationship between the radii of the iris border with the sclera and the iris border with the pupil. 34
Figure 6-3: Pupil correctly detected using Daugman's iris-pupil radii relation. 34
Figure 6-4: Pupil correctly detected in 'upper part of iris covered by eyelid' image using Daugman's iris-pupil radii relation. 35
Figure 6-5: Pupil correctly determined in 'upper part of iris with covered by eyelid' image of size 126 by 198 pixels using the Daugman's suggestion on how the iris and pupil radii are related. 36
Figure 7-1: (a) Original Image of eye (b) Histogram of original image of eye (c) Image of the eye after histogram equalization (d) Histogram of histogram equalized image of eye. 37
Figure 7-2: The integral/change in gradient value of the histogram equalized image at its centre point i.e. (x, y) = (86, 126) showing a steeper slope with a gradient of around 0.10, compared to non histogram equalized copy of the same image(as shown in Figure 4-2) having a smaller gradient equals to 0.09. 38
Figure 7-3: Output image showing two circles at the limbic border of the iris (the outer circle) and the border of the iris with the pupil (the inner circle). 39
Figure 7-4: Shows the result of the performance of Daugman's algorithm on a low contrast image. The iris is detected correctly. However, due to very low contrast between the iris and the pupil, the pupil border with iris is wrongly detected. 40
Figure 7-5: Shows the result of the performance of Daugman's algorithm on the same image with contrast enhanced. The iris is detected correctly. However due to a better contrast between the iris and the pupil, the pupil border with iris is also correctly detected. 41
Figure 8-1: (a) Input blur image that does not have a sharp iris to sclera and iris to pupil contrast (b) iris and pupil detected incorrectly 44
Figure 8-2: (a) Input noise image of light reflection (b) iris and pupil detected incorrectly 44
Figure 8-3: (a) Input noise image where the image of the is rotated at some angle (b) Iris and pupil incorrectly detected 44

List of Tables

Table 3-1: Output table that shows the X and Y center coordinates and the radius of the iris after processing the image with Daugman's operator. 23
Table 5-1: Shows the X and Y center coordinates and the radius of the iris outer border after processing the input image in Figure 5-6 with Daugman's operator using 50% lateral circumference pixels. 30
Table 5-2: Shows the X and Y center coordinates and the radius of the iris outer border after processing the input image in Figure 5-7 with Daugman's operator using 50% lateral circumference pixels. 30
Table 5-3: Shows the X and Y center coordinates and the radius of the iris after processing the input image in Figure 5-8 with Daugman's operator using 50% lateral circumference pixels. 31
Table 6-1: Shows the X and Y center coordinates and the radii of the iris and pupil after processing the image with Daugman's operator using 50% lateral circumferential pixels. 34
Table 6-2: Shows the X and Y center coordinates and the radii of the iris and pupil after processing the input image in Figure 5-7 with Daugman's operator using 50% lateral circumferential pixels. 35
Table 6-3: Shows the X and Y center coordinates and the radii of the iris and pupil after processing the input image in Figure 5-8 with Daugman's operator using 50% lateral circumference pixels. 36
Table 7-1: Shows the X and Y center coordinates and the radii of the iris and pupil after processing the Daugman's operator on the 'histogram equalized' image. 39

Chapter 1

1 Introduction

1.1 Biometric in general

In terms of computer science, the term biometrics refers to technologies that analyze and measure human body characteristics for the authentication purposes. These characteristics include fingerprints, DNA, voice patterns, irises, hand measurements and facial patterns. In this modern era, when internet has reached its peak and forms the basis for all modern banking and business systems [1], the accurate verification for accessing accounts is also becoming a necessity. A demand for a superior technology compared to passwords, secret questions and other access protecting technologies led to the increased research and development of biometrics. The biometric feature that is used in this thesis is an iris.

1.2 Iris biometric

Figure 1-1: Image of an eye representing the iris, pupil and sclera.

The iris biometric deals with identifying a human being by his/her iris pattern extracted from the images of his/her eye. As shown in Figure 1-1, the human eye consists of 3 major parts: pupil (the innermost black part), iris (the colored part) and sclera (the white part). The iris and pupil as said to be non-concentric [2]. The radius of inner border of the iris i.e. it's border with the pupil is also not constant since the size of pupil increases and decreases depending on the amount of light incident to the pupil. Every individual has a unique pattern of iris [2]. This pattern can be extracted from the image of the eye and encoded. The code can be compared to the codes obtained from the images of

other eyes or the same eye. The result of comparison can represent the amount of difference between the compared codes. In that way it can be concluded if the compared eye patterns belong to the same or different eye.

1.3 Iris compared to other biometrics

The notable advantage of iris biometric over other biometrics is that irises have enormous pattern variability [3]. According to John Daugman iris pattern conditional false reject probability is $10^{9.6}$ that is one in 4 billion [16]. A single iris scan can analyze more than 200 different points of the iris, such as furrows, corona, rings, freckles etc [4]. Compared to other biometrics, such as voice and facial features that tend to change over time, iris biometric is stable and remains the same for a person's lifetime [5]. The use of contact lenses, glasses and even eye surgery cannot affect the iris characteristics [6].

1.4 Overview of methods to segment iris

To successfully perform iris recognition, accurate iris segmentation is a very important prerequisite [7, 8]. Two widely used and well known methods of iris segmentation are Wilde's method and Daugman's method respectively. Wilde has proposed a two step iris segmentation method: 1) a binary edge map based on gradient based is constructed from the intensities of the pixels in an iris image, 2) the iris inner and outer borders are detected using Hough transform [9]. Daugman's algorithm, named after the professor John Daugman, is an integrodifferential operator that searches over an image of the eye for the circular pupil and the limbic borders of the iris. It is a circular edge detector that searches for the parameters of a circular border. The sum of circumferential pixel intensity values at this circular border should have the maximum change in values compared to a one pixel radius wider circular region away from the same center pixel, as for the circular border. Daugman's algorithm for iris segmentation is used in this thesis.

Chapter 2

2 Daugman's algorithm description

2.1 Daugman's operator:

The task is to find the centre coordinates and the radius of the iris and the pupil and Daugman's equation is employed for this task. The centre point of Daugman's theory of border recognition is the integrodifferential equation as follows [11]

$$\max_{(r,x_0,y_0)} \left| G_\sigma(r) * \frac{\partial}{\partial r} \oint_{r,x_0,y_0} \frac{I(x,y)}{2\pi r} ds \right| \quad . \qquad (1)$$

I(x, y) is the intensity of the pixel at coordinates *(x, y)* in the image of an iris.
r denotes the radius of various circular regions with the center coordinates at *(x0, y0)*.
σ is the standard deviation of the Gaussian distribution.
$G_\sigma(r)$ denotes a Gaussian filter of scale sigma (σ).
(x_0, y_0) is the assumed centre coordinates of the iris.
s is the contour of the circle given by the parameters (*r, x0, y0*).

2.2 Two dimensional 2D Gaussian filter

In electronics and signal processing, a Gaussian filter is a filter whose impulse response is a Gaussian function. Mathematically, a Gaussian filter modifies the input signal by convolution with a Gaussian function [12] [13] [14]. In our thesis, the Gaussian smoothing operator is a 2-D convolution operator that is used to smooth the images of the eye in order to remove noise.

The one-dimensional Gaussian filter has an impulse response given by

$$g(x) = \sqrt{\frac{a}{\pi}} . e^{-a.x^2} \qquad (2)$$

where ‘a’ denotes the height of the curve's peak (magnitude of the impulse response) and has a value greater than zero.

In two dimensions, it is the product of two such Gaussians, one per direction:

$$g(x,y) = \frac{1}{2\pi\sigma^2} e^{-\frac{x^2+y^2}{2\sigma^2}} \quad (3)$$

where x and y denote the distance from the origin towards the edges of the filter in the horizontal axis and vertical axis directions, respectively and σ is the standard deviation of the Gaussian distribution [12, 13, 14].

The Gaussian filter in our case is designed in MATLAB and is a 1 by 5 (rows by columns) vector with intensity values given by vector A = [0.0003 0.1065 0.7866 0.1065 0.0003]. The designed filter is shown in Figure 2-1.

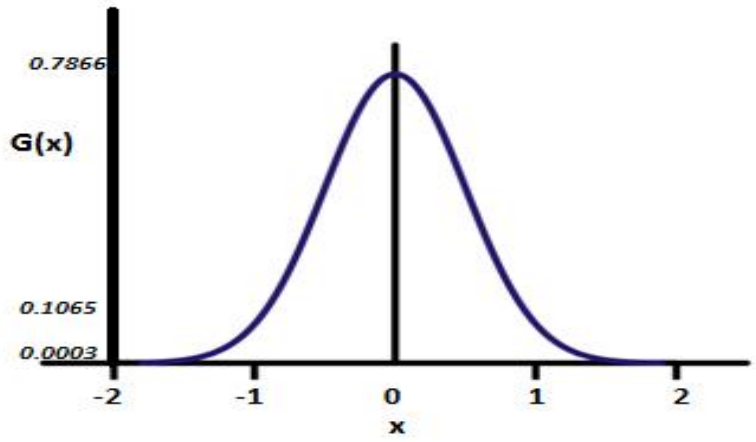

Figure 2-1: Graph of the 1D Gaussian filter as used in the thesis.

2.3 Two dimensional 2D convolution

In mathematics and, in particular, functional analysis, convolution is a mathematical operation on two functions f and g, producing a third function that is typically viewed as a modified version of one of the original functions [15].

$$(f * g)(t) = \int_{-\infty}^{\infty} f(\tau) g(t - \tau) d\tau \qquad (4)$$

While the symbol *t* is used above, it need not represent the time domain.

2.4 The Daugman's operator explained

The operator searches for the circular path where there is maximum change in pixel values, by varying the radius 'r' and the center (x, y) of the circular contour. The operator is applied iteratively with the amount of smoothing progressively reduced in order to obtain accurate localization. Assuming that the variables x, y and r belong to the ranges [0; X], [0; Y] [0; R] respectively, this method has the computational complexity of order [X × Y × R]. Thus, at every pixel, a total of R scans are necessary to compute the circle parameters using this approach.

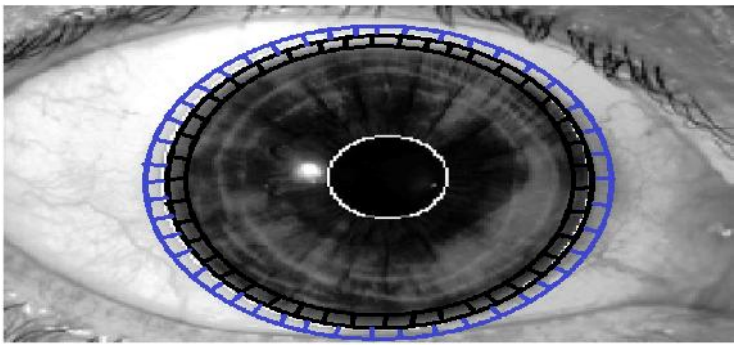

Figure 2-2: The black boxed line represents one pixel wide iris border at a certain radius 'R' (not to scale) at the centre coordinate and the blue boxed line represents one pixel wide circle at the same center coordinate at radius 'R+1'.

A search over the entire image (of an eye) is done, pixel by pixel. At every pixel, the *normalized* sum of all circumferential pixel values, at increasing radius is found. At every level of increased radius, the difference between the *normalized* sums of pixel intensity values at adjacent radii circle (see Figure 2-3) is noted. After the entire search, summation and differentiation in the calculating process, that pixel is stated to be the centre pixel of the iris where the change in sum of circumferential pixels intensity values between two adjacent contours is the greatest.

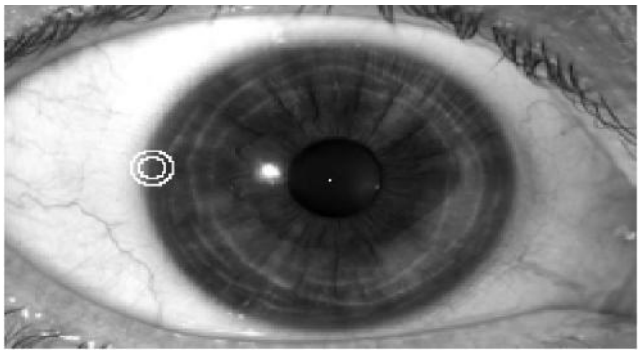

Figure 2-3: Two white circles representing two contours that are 1 pixel radius apart representing the concept of 'adjacent radii circles'.

Chapter 3

3 The enhancement of an eye image before the application of the Daugman's operator

3.1 Countering the effect of light reflection on images

Light reflections in the eye images negatively affect iris border detection by means of Daugman's algorithm. The white spot in Figure 3-1a) and the 'white region' in Figure 3-1b) indicated by the dotted blue circles show the light reflections in the eye images. These light reflections cover the parts of the eye image causing hindrance in the iris detection process. As can be observed, the 'light reflection affected region' is a region consisting of the pixels with high intensity values (since it is a white region). The region surrounding it is a region consisting of the pixels with low intensity values (since it is a darker region). This element of light reflections on eye images affects the iris detection in two ways. Firstly, the original pixel intensity values have been replaced by the higher intensity values in the part of the image, affected by light reflection. Therefore the original information of this part of the image has been lost. Secondly, as apparent in Figure 3-1a) and 3-1b), there is an observable difference in intensity values between this 'light affected region' and it's surrounding darker region.

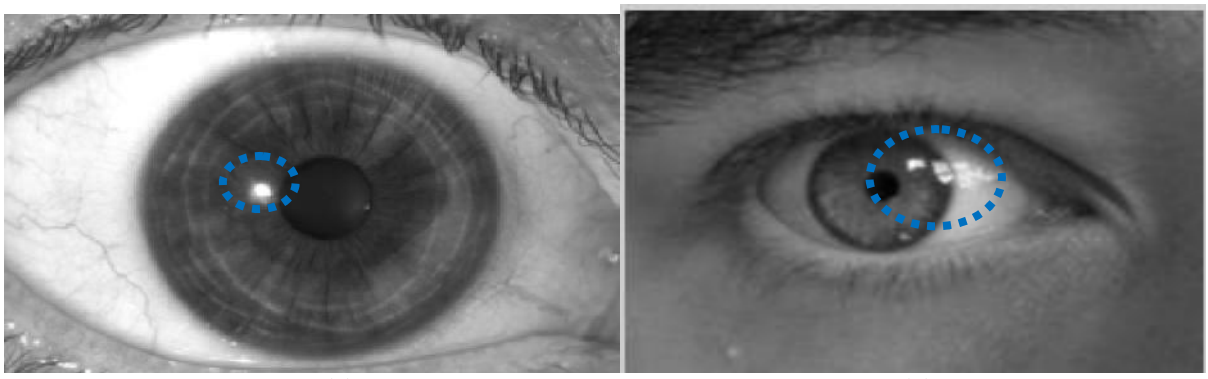

(a) **(b)**

Figure 3-1: (a) Light reflection affected eye image of size 164 by 246 pixels (b) Light reflection affected eye image of size 178 by 238 pixels.

Daugman's operator applied to such images detects the intensity change at this reflection affected white regions to be the maximum change in sum of circumferential pixels intensity values. Hence due to this element of light reflection the iris and pupil borders are incorrectly identified as shown in figure 3-2a) and 3-2b).

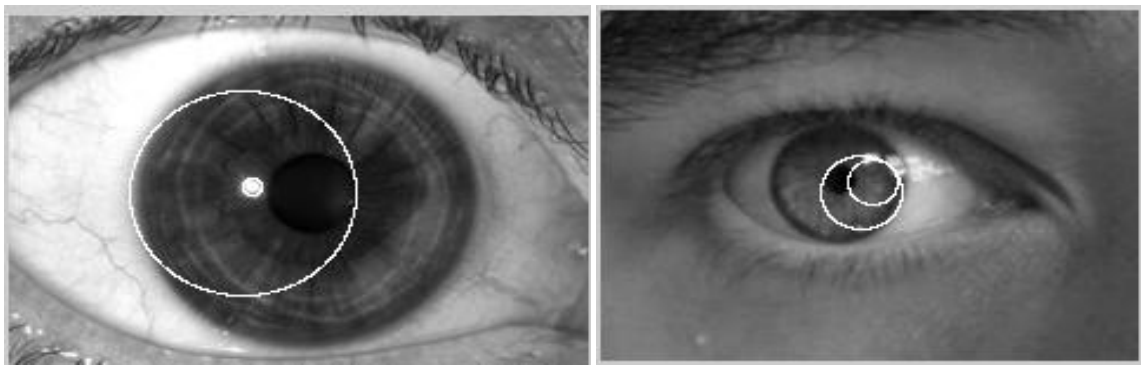

(a) **(b)**

Figure 3-2: (a) Iris and pupil wrongly detected for light reflection affected image for the input image shown in Figure 3-1(a) (b) Iris and pupil wrongly detected for light reflection affected image as shown in Figure-3-1(b).

In order to avoid light reflection affecting the iris detection, a morphological operator is used. The operator fills in the light affected regions with the average of intensities of pixels from the region surrounding it. The MATLAB commands 'imcomplement' and 'imfill' are applied to the image before applying the Daugman's operator.

The command 'imfill' fills holes in the grayscale image. In this thesis, a hole is defined as an area of dark pixels surrounded by lighter pixels i.e. a pixel of lower intensities surrounded by pixels with the higher intensities. However in our case, the region that needs to be filled is a high intensity region and is surrounded by a low intensity region. The MATLAB command 'imcomplement' is applied first to make dark areas lighter and light areas darker. This procedure can be considered as taking the negative of the particular eye image. This complemented image is then processed by the morphological operator 'imfill' that fills in this dark region (the light affected region in the original image) with intensity similar to that of its neighborhood. Using 'imcomplement' again reverses the dark region into lighter region and vice versa. This command removes specular reflections due to light in the image.

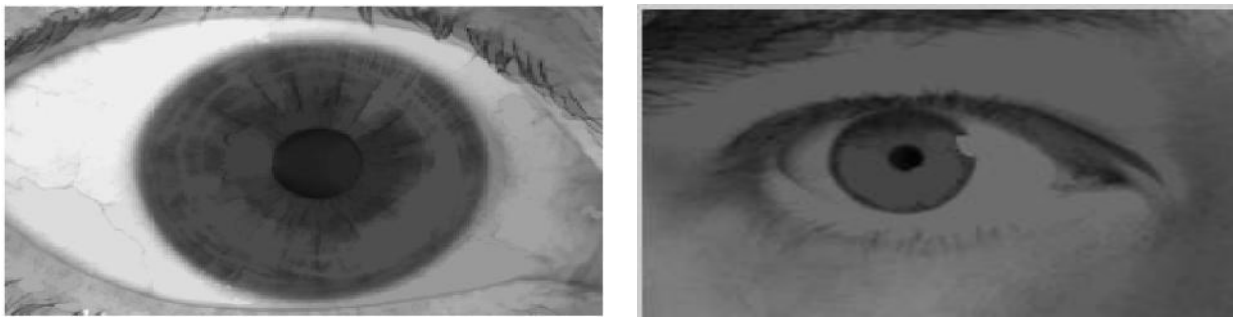

(a) (b)

Figure 3-3: (a) Output for the input image as shown in Figure 3-1(a) after the morphological operation (b) Output for the input image as shown in Figure 3-1(b) after applying the morphological operation

The images in Figure 3-3 (a) and (b) show the results after using the morphological operators on the 'light reflection affected' images in Figures 3-1(a) and (b). From the Figures3-3(a) and (b) it can be observed that the light affected region has been removed to a great extent.

3.2 Thresholding

Thresholding is a method of image segmentation. The concept of 'thresholding below' is used before implementing Daugman's equation. 'Thresholding below' marks some pixels as 'object pixels' if those pixels have an intensity value below a certain threshold value. This is done assuming that the 'object pixels (i.e. the pixels that could possibly be the centre pixels)' to be darker than the background pixels. Having a look at the gray scale image of an eye, one can assume that the centre pixels for both the iris and the pupil lie inside the 'dark' pupil region. In some case, the centre pixels might lie in the comparatively lighter region of the iris but not in the white sclera region. A range of [0;1] for intensity values of the pixels in the eye images has been used, where 0 represents the absence of the light (black pixels) and the pixel with full intensity (white pixel) has intensity value equal to 1. In our case, the object pixels (i.e. the pixels that could possibly be the centre pixels) have been assumed to have a value below 0.5. So, all the pixels that have an intensity of less than 0.5 are marked and the Daugman's operator is applied on those pixels only.

3.3 Detecting pixels with locally minimal intensity values (local minima pixels)

The threshold image is further scanned, pixel by pixel to determine whether the pixel is a local minimum in that particular pixel's immediate 3-by-3 neighborhood. This means that every pixel intensity is compared to the intensities of the pixels in its immediate nine neighborhood pixels. The pixel with the lowest intensity value amongst these nine pixels is used for further calculations. The rest of the pixels are discarded.

The reduction of the number of object pixels, on which the Daugman's operator is applied, makes the iris detection process faster. For example, in the eye image as shown in Figure 1-2, the total number of pixels that 40344 (164 by 246 image size). After masking the image with the local minima operator and thresholding the number of object pixels left is 922 pixels.

3.4 No circles outside the image

The iris border is expected to lie completely inside the input image. During the iris detection process, for every assumed center pixel the sum of values of circumferential pixels is noted at different levels of radii. Therefore those circular regions of pixels that do not completely lie inside the eye image are neglected. This means that for a assumed center pixel, the circular contour search is stopped at the radius at which a complete circle of pixels is unable to be formed since the contour pixels coordinates lie outside the coordinates range limited by the image dimensions.

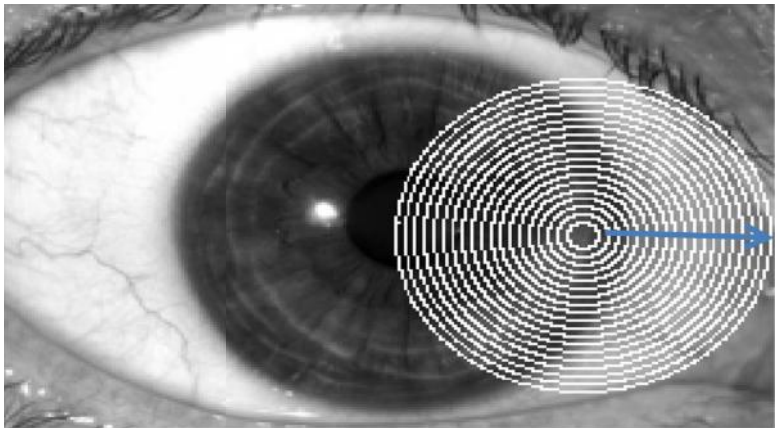

Figure 3-4: Image showing the different circular contours at a range of radii.

This process decreases the number of calculations. Therefore the time which is necessary to segment the image of the iris is reduced.

3.5 Result

The white spots shown in Figure 3-5 represent those pixels that are considered to be the possible centre pixels of an iris outer border for this particular image. The four procedures to enhance the image and speed up the segmentation process are listed once again below:

1. The morphological operation using MATLAB tool 'imfill'
2. Thresholding
3. Identifying local minimum point in 3x3 neighborhood
4. Cutting off those circles that do not fit inside the image.

These changes help to improve the efficiency of the Daugman's operator in avoiding the effect of light reflection and making the process faster by reducing the number of pixels to work on.

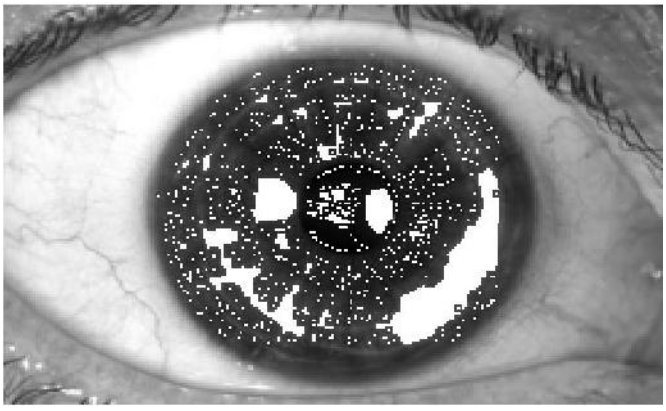

Figure 3-5: Image showing object pixels after thresholding and local minima pixel detection.

Daugman's operator has been applied to the eye image processed by the morphological operators as shown in Figure 3-3(a) and only on the object pixels shown by the white spots in Figure 3-5. The result of the application of the operator is the correctly detected iris border as shown in Figure 3-6.

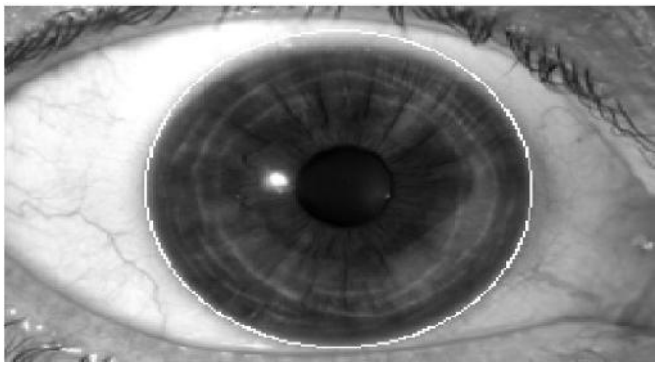

Figure 3-6: Output image that shows limbic border of the iris (the white circle).

	X coordinate	Y coordinate	Radius
Iris	85	127	73

Table 3-1: Output table that shows the X and Y center coordinates and the radius of the iris after processing the image with Daugman's operator.

Chapter 4

4 Plotting the results of the performance of the Daugman's operator

4.1 Graph of sum of circumferential pixels intensity values for the detected iris border

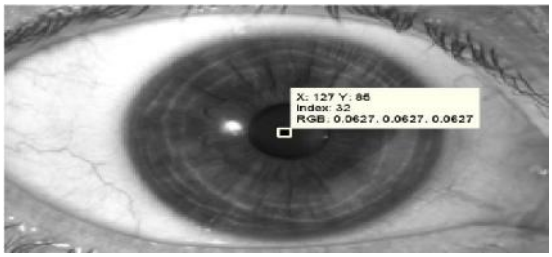

Figure 4-1: Image of the eye indicating the calculated centre pixel with coordinates (X, Y) = (127, 85)

The image of the eye in Figure 4-1 shows the centre pixel for the particular grayscale image. The coordinates for the center pixel are calculated (see Figure 3-5 and Table 3-1) to be X=127 and Y=85. The graph in Figure 4-2 shows the 'normalized sum of circumferential pixel intensity values' at the range of radii of 25 to 75 at this calculated centre pixel.

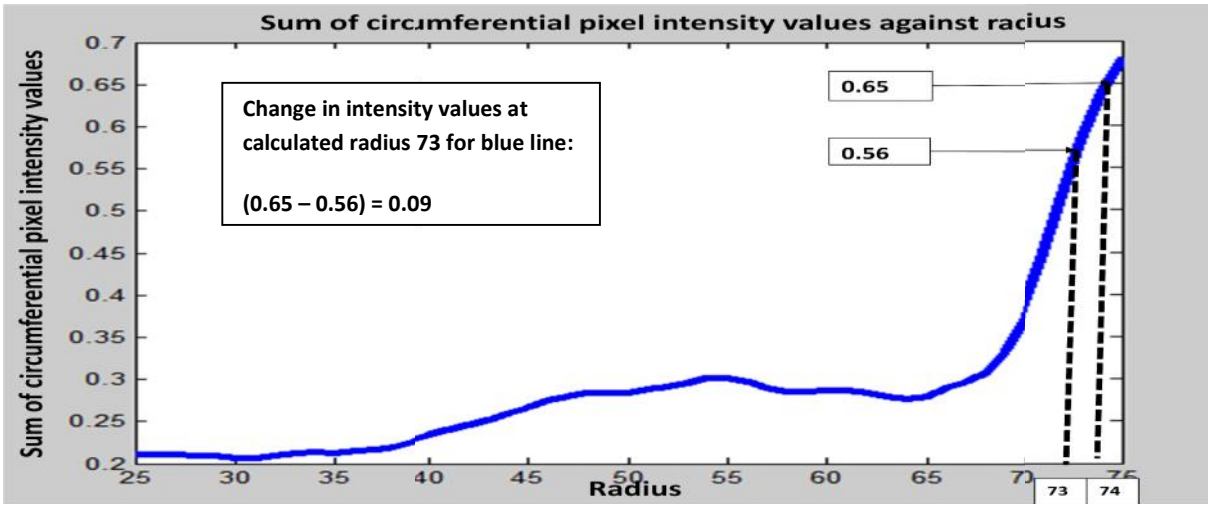

Figure 4-2: Graph shows the dependence of the sum of circumferential pixel intensity values versus radius for a center pixel, shown in Figure 4-1.

This graph shows the maximum change in the normalized sum of circumferential pixel intensity values between the calculated radius for the image i.e. 73 pixels and its immediate 1 pixel wider radius i.e. 74 pixels. This change in the normalized sum of circumferential pixel intensity values is

calculated to be 0.09 between the two radii. This is the highest difference in such sums for two circular regions that are one pixel apart.

4.2 Graph of sum of circumferential pixels intensity values for a pixel near the detected iris outer border

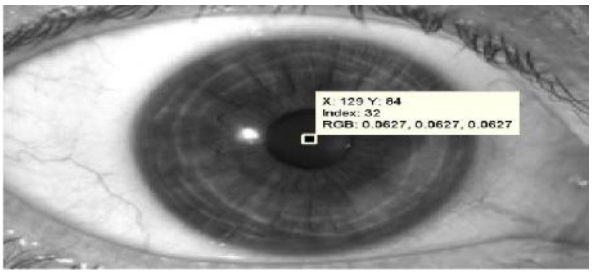

Figure 4-3: Image of the eye indicating a pixel near the centre pixel with coordinates (X, Y) = (129, 84)

The image of the eye in Figure 4-3 represents 'a pixel near the calculated centre pixel' for the particular grayscale input image. The coordinates for this particular pixel are X=129 and Y=84. The graph in Figure 4-4 shows the 'normalized sum of circumferential pixel intensity values' at the range of radii of 25 to 75 at this particular pixel.

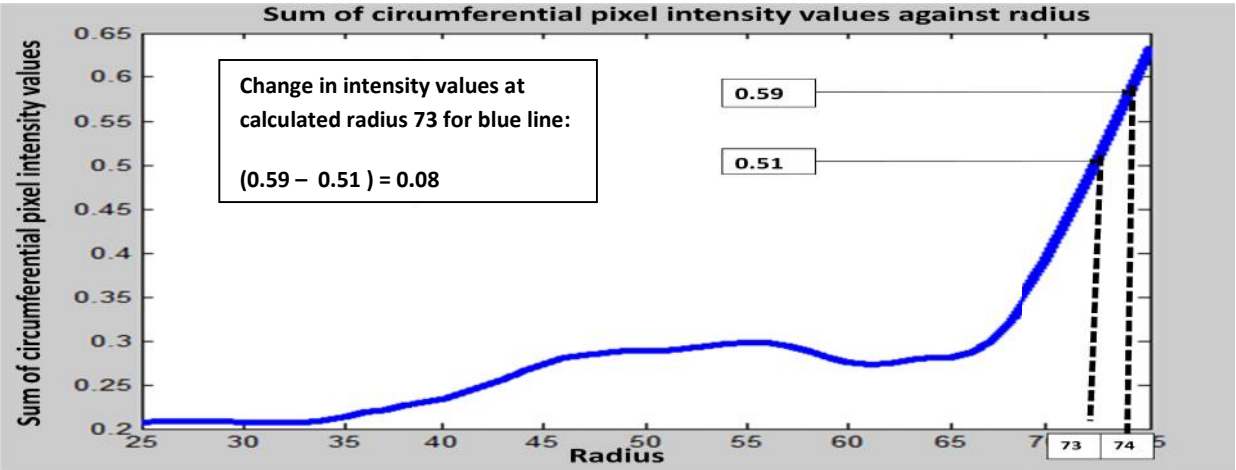

Figure 4-4: Graph at the pixel in figure 4-3 (a pixel near the centre of the iris), of the change in sum of circumferential pixel intensity values against increase in radius.

This graph shows the greatest difference in the normalized sum of circumferential pixel intensity values between the calculated radius for the image i.e. 73 and its immediate 1 pixel wider radius i.e. 74. This change in the normalized sum of pixel intensity values which is calculated to be 0.08 is smaller compared to the gradient found at the same radii, to be equal to 0.09 for the calculated center pixel of the eye as shown in Figure 4-2.

Chapter 5

5 Effect of the covering of the part of an eye image by an eyelid on the Daugman's operator performance

Figure 5-1: image with upper part of the iris covered by the eyelid.

In the eye images used in previous sections, the iris part of the eye was fully visible and no part of the iris had been covered by the eyelids. The application of the Daugman's algorithm on such images resulted into correctly detected irides (see section 3.6).The problem occurred in an eye image where the upper and/or part of the iris border had been partly covered by the eyelid as shown in Figure 5-1. Daugman's operator applied to such an image identified the iris border incorrectly, as shown in Figure 5-2. This failure can be explained by the fact that some pixel intensity values at the iris border had been covered by the eyelid and could not be included into calculations.

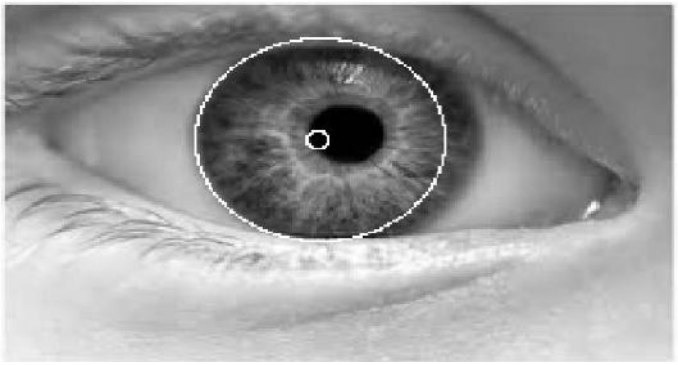

Figure 5-2: Iris wrongly detected using Daugman's operator on the image with upper part of the iris covered by the eyelid as shown in Figure 5-1.

5.1 Daugman's suggestion to solve 'occlusion by eyelid' problem

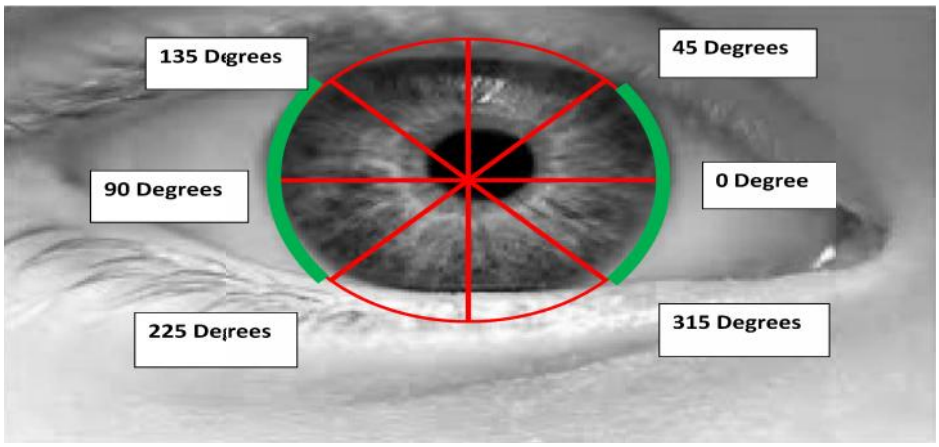

Figure 5-3: 50% (25% lateral left and 25% lateral right) of the circumference at the specified angles, to be used for iris border estimations, shown by the green arcs.

For the pupil iris border detection the use of Daugman's operator is appropriate even in the eye images where the eyelids may be covering part of the iris. This is true as far as the entire pupil and at least one pixel radius wide circular region of the image outside the pupil is visible in the image. This case is not the same for the iris. If the iris is covered wholly or partly by the eyelid, reading intensity values from the eyelid covered parts of the iris may not be possible. Hence Daugman changed his approach for detecting the iris border in images where the iris border is partly covered. Daugman suggested changing the path of contour integration from circular to an arc [11]. His suggestion makes use of only the lateral portions to mitigate the effect of occlusions that might occur at the top and/or at the bottom.

Daugman suggested using 50% of the pixels for the sum of circumferential pixel intensity values in every contour's circumference. These 50% of pixels should be the pixels at angles of 0 to 45 degrees, 135 to 225 degrees and 315 to 360 degrees as shown by the green lines in figure 5-3, for all contours at every centre pixel. This suggestion has been tested to be very efficient for images that have their upper and/or lower parts of their irides partly covered by their eyelids (as shown in the Figure 5-3). On the other hand, this suggestion fails for images of eye taken while the person's head is tilted at some angle or images whose left and right portions of the iris might also be covered.

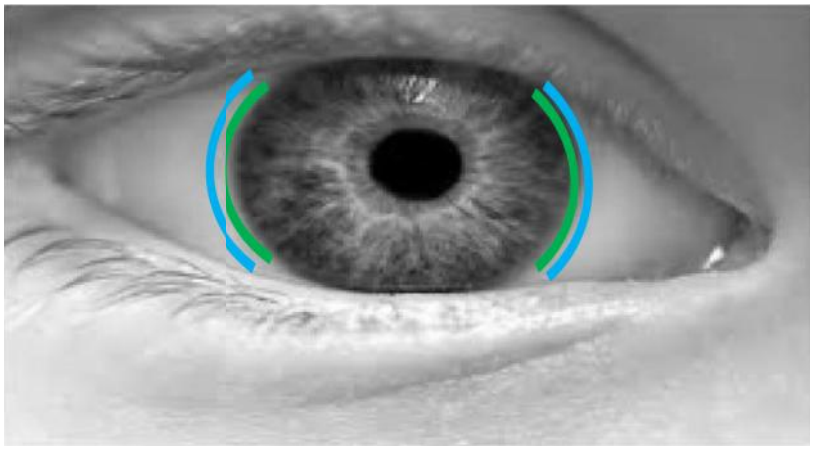

Figure 5-4: Daugman's assumption to use the proposed 50 % circumference. The green and blue arcs represent the iris border at radius 'R' and 'R+1'.

Daugman's suggestion of using the 50% circumferential pixels can only be used if the maximum change in normalized sum of circumferential pixels intensity values between two circular arcs is assumed to indicate the iris border. In addition to that, the iris border at these angles (as shown in Figure 5-3) must also be visible in the eye image.

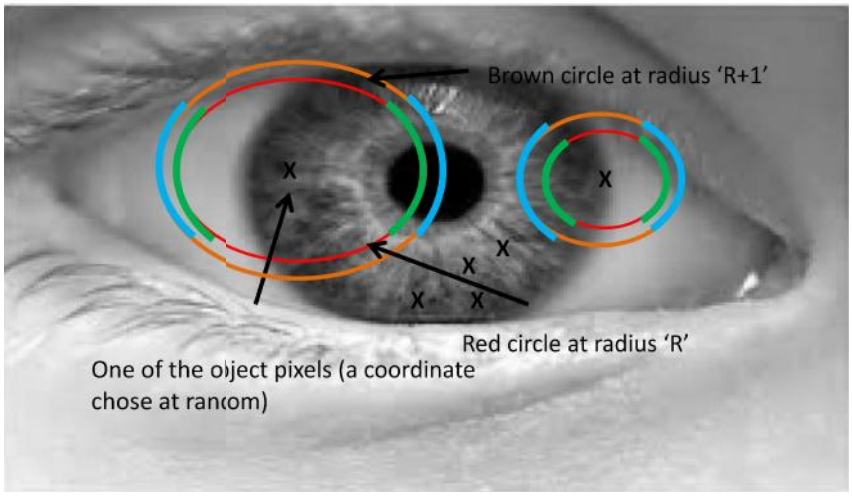

Figure 5-5: At every object pixel denoted by 'X' (not all object pixels shown), calculations at increasing radius, at every two adjacent radii (i.e. R & R+1) as shown by the red and brown circles, only the pixels in green arc are subtracted by the pixels in blue arc for calculations.

The similar procedure is repeated for searching for the maximum change in circumferential pixels intensity values at increasing radius. However intensity values only from pixels in the lateral portions (as shown by the green and blue arcs in Figure 5-5) are used to calculate this change.

5.2 Results obtained by using Daugman's suggestion to solve 'occlusions by eyelid' problem

The Figures 5-6 and 5-7 show the correct detection of the iris borders using Daugman's 50% circumferential pixels approach on eye images that have their iris partly covered. The Tables 5-1 and 5-2 show the X, Y centre coordinates and the radius for eye images shown in Figures 5-6 and 5-7 respectively. As shown by the following images, the irides for all such images are apparently detected correctly (as the detection circle appears to be on the iris border) using Daugman's 50% circumferential pixel value assumption (see section 5.1).

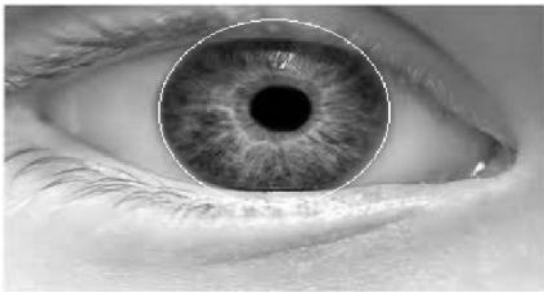

Figure 5-6: Iris outer border correctly determined in 'iris covered by eyelid' image using 50% circumference

	X coordinate	Y coordinate	Radius
Iris	62	125	53

Table 5-1: Shows the X and Y center coordinates and the radius of the iris outer border after processing the input image in Figure 5-6 with Daugman's operator using 50% lateral circumference pixels.

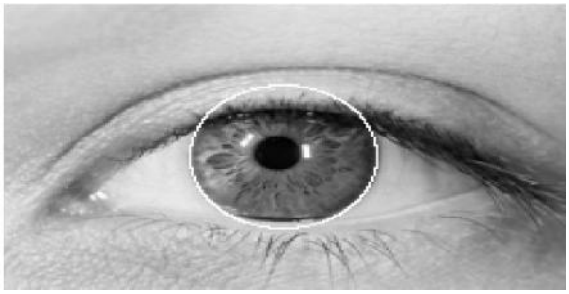

Figure 5-7: Iris outer border detected in 'iris covered by eyelid' image of size 153 by 228 pixels using 50% circumference.

	X coordinate	Y coordinate	Radius
Iris	82	114	38

Table 5-2: Shows the X and Y center coordinates and the radius of the iris outer border after processing the input image in Figure 5-7 with Daugman's operator using 50% lateral circumference pixels.

Figure 5-8: Iris outer border detected in 'iris covered by eyelid' image of size 126 by 198 pixels using 50% circumference.

	X coordinate	Y coordinate	Radius
Iris	57	93	33

Table 5-3: Shows the X and Y center coordinates and the radius of the iris after processing the input image in Figure 5-8 with Daugman's operator using 50% lateral circumference pixels.

5.3 Failure to solve 'occlusion by eyelid' problem using the Daugman's suggestion

According to Daugman, images with less than 50% of the iris visible between the fitted eyelids splines are deemed inadequate, e.g., in blink [5]. Daugman's suggestion performed iris detection effectively in the images as shown in Figures 5-7 and 5-8 where only the upper and/or lower parts of the iris borders were partly covered by the eyelids. On the other hand, Daugman's 50% circumference approach caused unsuccessful iris detection when the eyeball in the input eye image was shifted at some angle. Figure 5-9(a) shows the image of an eye in which the eyeball has a shift in angle to the left. Figure 5-9(b) shows the output image for the 'eyeball shifted image' where the iris has been wrongly detected. Daugman's suggestion also proved to be ineffective with images having other sorts of noise. (See chapter 8)

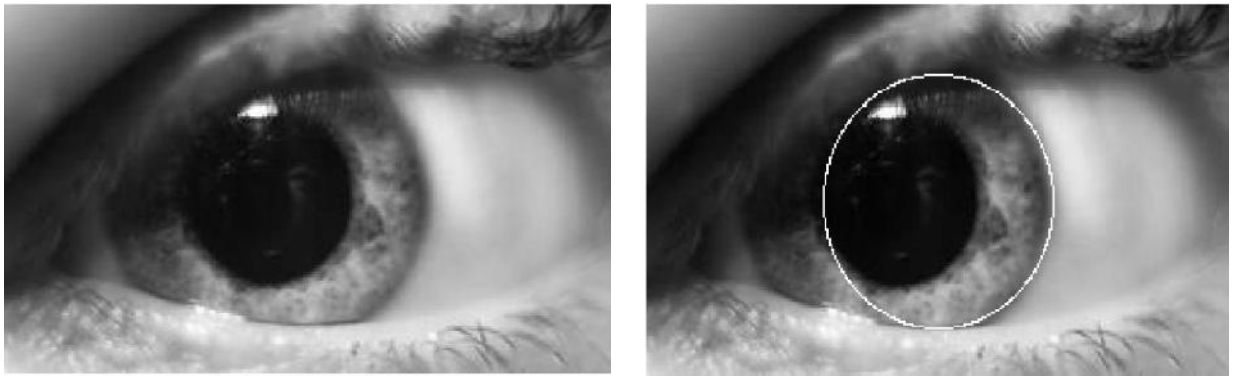

Figure 5-9: (a) Eyelid covered image of size 171 by 294 pixels with the eyeball moved to an angle such that most of the upper, the lateral left portion and most of the lower part the iris border are covered by the eyelid (b) Iris incorrectly determined using 50% circumference approach.

Daugman's suggestion of using 50% circumferential pixels failed to work once the eyeball moved at some angle and the eyelid covered a part of the left and/or right portions of the iris border. The image in Figure 5-10 shows that 25% lateral right sided portion of the iris border (as shown by the arc in green to the right) is completely visible. However the 25 % lateral left sided iris border is partly covered by the eyelid. In order for Daugman's suggestion to solve the eyelid problem successfully, the lateral left and right 50% circumference of the iris border should be completely visible (see Figure 5-3).

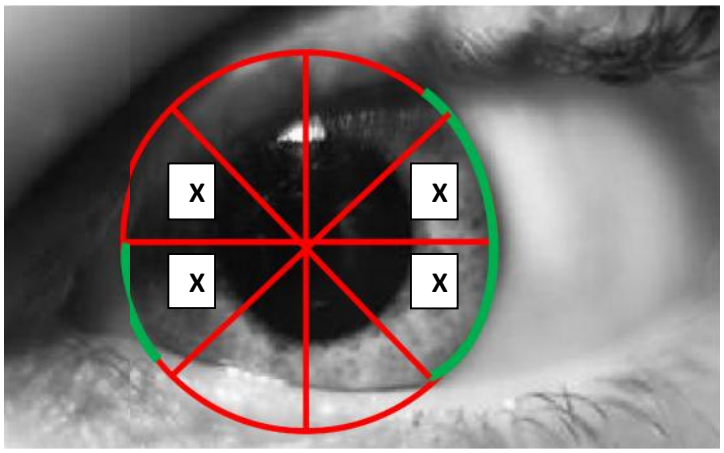

Figure 5-10: Image representing the tilted angle showing that only 3/8th of the iris border is visible since the eyeball has a shift to the left.

Chapter 6

6 Pupil detection (iris-pupil radii relation)

Once the iris outer border has been detected, the pupil's centre coordinates are found by searching the 10x10 neighborhood around the iris centre. For each pixel in this neighborhood a range of radii is used until a maximum difference in the sum of circumferential pixel intensity values between two circular regions, one pixel radius apart, is found [11]. Once again all the pixels in the image after thresholding are used to search for the pupil centre coordinates and its border as done previously for the iris outer border. Daugman's approach that the non co-centric iris and pupil centre coordinates lie within a 10x10 neighborhood to each other, narrowed down the search area and made the search process faster.

The detection of the iris border greatly constrains the pupil border search area. Concentricity of these boundaries cannot be assumed [11]. Very often the pupil center is nasal and inferior to the iris center. Thus, three parameters namely the x, y centre coordinates and the radius of the pupil border defining the pupillary circle must be estimated separately from those of the iris outer border [11]. According to Daugman, the pupil radius lies in a range of 10 to 80 percent of the iris outer border radius as shown in Figure 6-1.

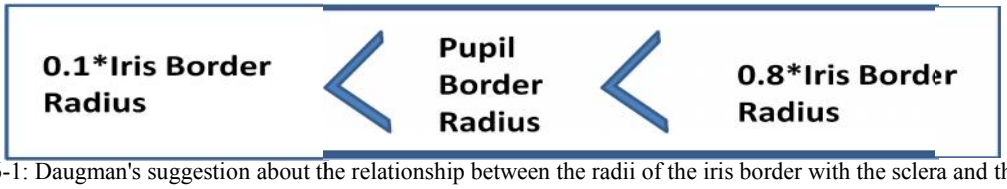

Figure 6-1: Daugman's suggestion about the relationship between the radii of the iris border with the sclera and the iris border with the pupil.

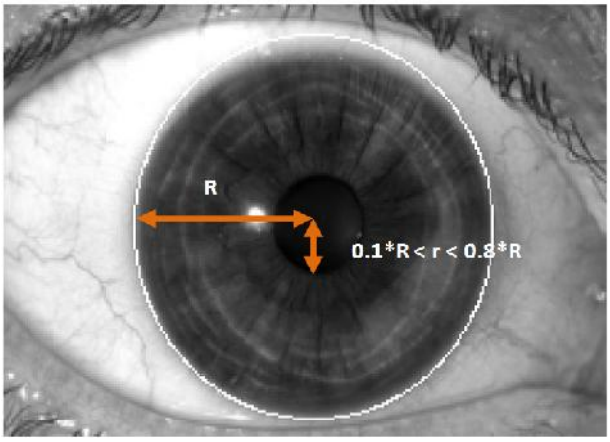

Figure 6-2: Daugman's suggestion about the relationship between the radii of the iris border with the sclera and the iris border with the pupil.

For example, the image shown in Figure 3-6 and its corresponding data stated in Table 3-1 show that the radius of the iris outer border is estimated to be 73 pixels. According to Daugman's approach as described above, the pupil border must lie in a range of (0.1*73) and (0.8*73) that is the range is between 7 and 58 pixels.

6.1 Results for pupil and iris detection

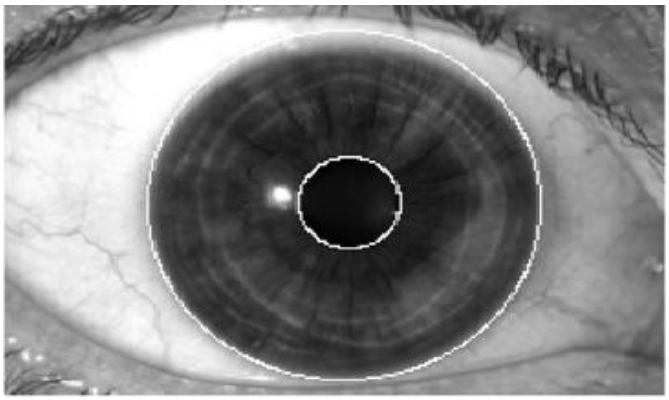

Figure 6-3: Pupil correctly detected using Daugman's iris-pupil radii relation.

	X coordinate	Y coordinate	Radius
Iris	85	127	73
Pupil	84	129	19

Table 6-1: Shows the X and Y center coordinates and the radii of the iris and pupil after processing the image with Daugman's operator using 50% lateral circumferential pixels.

As the Table 6-1 shows the radius calculated for the outer iris border is 73 pixels and the radius for the iris border with the pupil is calculated to be 19 pixels. This shows that the pupil radius is around 0.26 times smaller than the radius of the iris outer border shown in Figure 6-3. As shown in Figure 6-3, the pupil border is apparently detected correctly (as the white circle for pupil detection appears to be on the pupil border). The radius of the pupil border for this eye image does lie in the range 10% to 80% of the iris border radius (in this case 26%). Hence Daugman's suggestion relating the radii of the outer and inner iris borders as described in section 6 is proved to be correct.

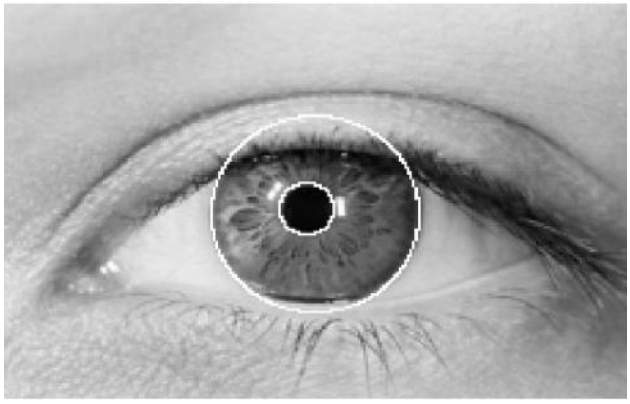

Figure 6-4: Pupil correctly detected in 'upper part of iris covered by eyelid' image using Daugman's iris-pupil radii relation.

	X coordinate	Y coordinate	Radius
Iris	82	114	38
Pupil	80	111	10

Table 6-2: Shows the X and Y center coordinates and the radii of the iris and pupil after processing the input image in Figure 5-7 with Daugman's operator using 50% lateral circumferential pixels.

As the Table 6-2 shows the radius calculated for the outer iris border is 38 pixels and the radius for the iris border with the pupil is calculated to be 10 pixels. This shows that the pupil radius is around 0.26 times smaller than the radius of the iris outer border shown in Figure 5-7. As shown in Figure 6-4, the pupil border is apparently detected correctly (as the white circle for pupil detection appears to be on the pupil border). The radius of the pupil border for this eye image does lie in the range 10% to 80% (in this case 26%) of the iris border radius. Hence, Daugman's suggestion relating the radii of the outer and inner iris borders as described in section 6 is proved to be correct.

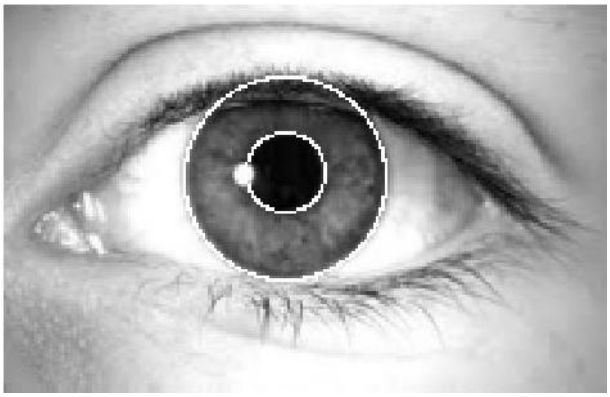

Figure 6-5: Pupil correctly determined in 'upper part of iris with covered by eyelid' image of size 126 by 198 pixels using the Daugman's suggestion on how the iris and pupil radii are related.

	X coordinate	Y coordinate	Radius
Iris	57	93	33
Pupil	55	93	13

Table 6-3: Shows the X and Y center coordinates and the radii of the iris and pupil after processing the input image in Figure 5-8 with Daugman's operator using 50% lateral circumference pixels.

As the Table 6-3 shows the radius calculated for the outer iris border is 33 pixels and the radius for the iris border with the pupil is calculated to be 13 pixels. This shows that the pupil radius is around 0.39 times smaller than the radius of the iris outer border shown in Figure 5-8. As shown in Figure 6-5, the pupil border is apparently detected correctly (as the white circle for pupil detection appears to be on the pupil border). The radius of the pupil border for this eye image does lie in the range 10% to 80% (in this case 39%) of the iris outer border radius. Hence Daugman's suggestion relating the radii of the outer and inner iris borders as described in section 6 is proved to be correct.

Chapter 7

7 Image enhancement techniques

Several image enhancement techniques have been used, such as contrast enhancement and histogram equalization, to enhance the input image before applying the Daugman's operator.

7.1 Histogram equalization

Histogram equalization is a technique that improves the contrast of images and it has been found to be one of the most powerful methods in image enhancement [17].

The steps for histogram equalization are:

1. It takes the cumulative histogram of the image for equalization.
2. Normalize the cumulative histogram to 255 (which is the maximum intensity value in the range (0 to 255) of a grayscale image).
3. Normalized cumulative histogram is used as the mapping function of the original image.

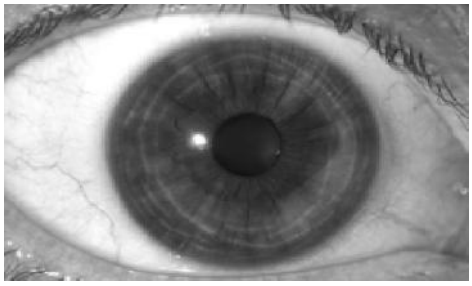

(a)

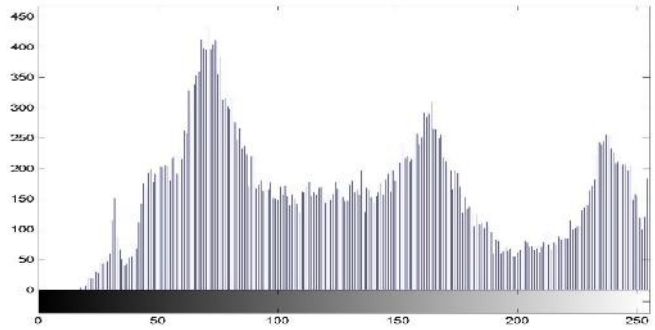

(b)

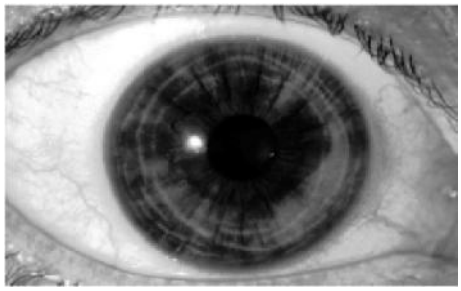

(c)

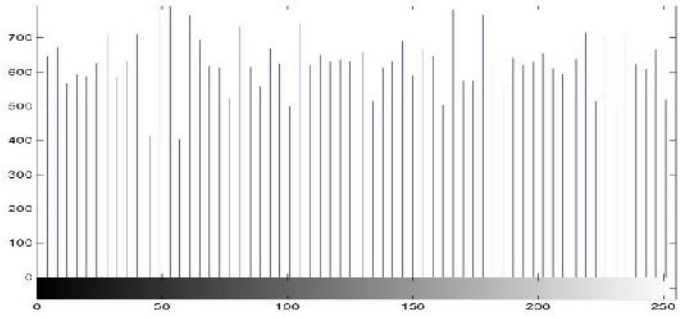

(d)

Figure 7-1: (a) Original Image of eye (b) Histogram of original image of eye (c) Image of the eye after histogram equalization (d) Histogram of histogram equalized image of eye.

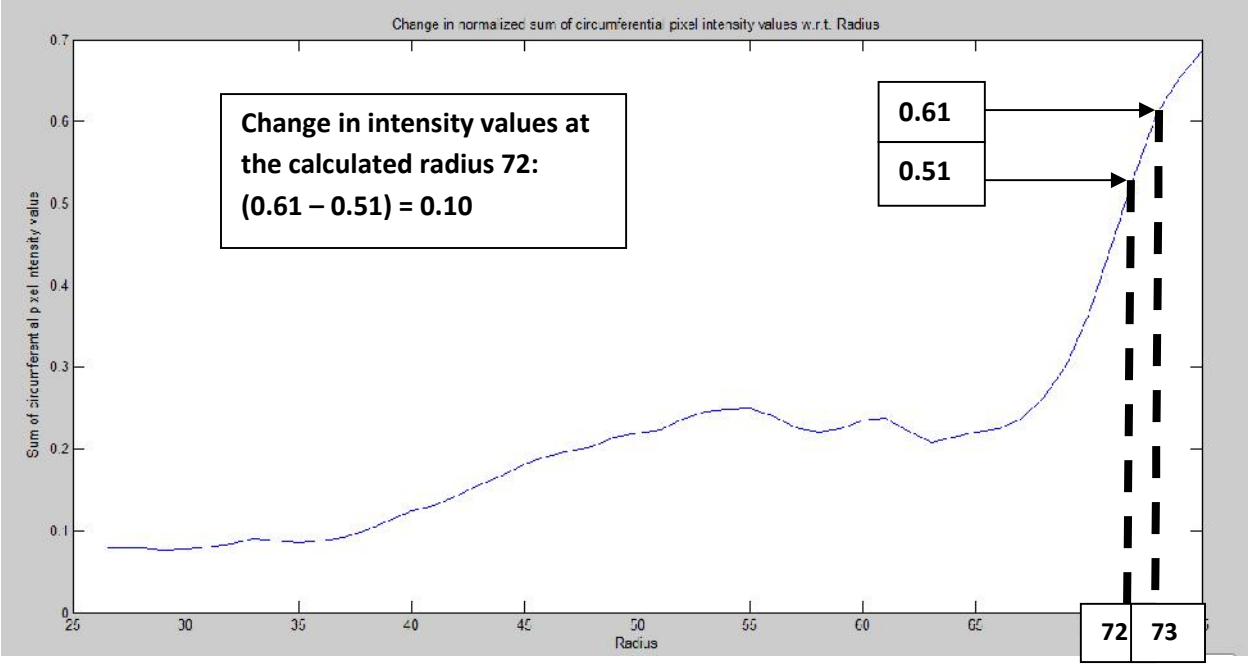

Figure 7-2: The integral/change in gradient value of the histogram equalized image at its centre point i.e. (x, y) = (86, 126) showing a steeper slope with a gradient of around 0.10, compared to non histogram equalized copy of the same image(as shown in Figure 4-2) having a smaller gradient equals to 0.09.

The histogram equalization of the eye image caused a change in intensity values of all pixels as well as the centre pixel of the image. Applying Daugman's operator on this enhanced eye image, a new pixel was calculated to be the centre pixel and a new radius was calculated for the iris outer border. As the graph in Figure 7-2 shows, for the new centre pixel (at radius 72), a greater difference in the sum of circumferential pixels intensity values at its iris outer border is estimated to be 0.10. This difference for the non-histogram equalized copy of the same image (as shown in figure 4-2) had been calculated to be equal to 0.09 which is smaller than 0.10. Histogram equalization normalizes the intensity values of all pixels in an image by allowing areas of lower contrast to have a higher contrast. Hence a greater change in sum of circumferential pixels intensity values at the iris outer border of the enhanced image was expected and a similar result has been observed in the graph above.

Result for the histogram equalized image

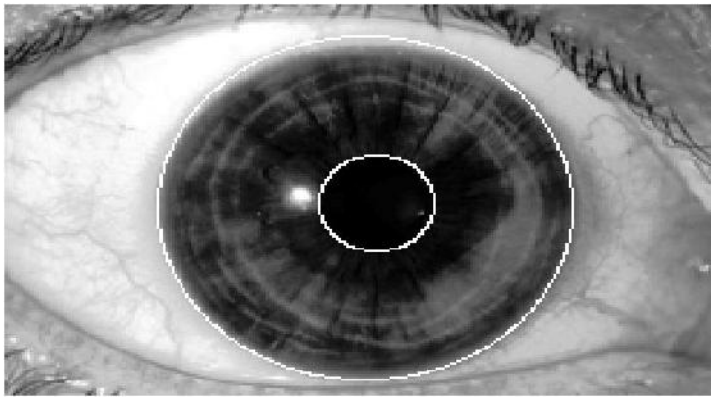

Figure 7-3: Output image showing two circles at the limbic border of the iris (the outer circle) and the border of the iris with the pupil (the inner circle).

	X coordinate	Y coordinate	Radius
Iris	86	126	72
Pupil	84	130	20

Table 7-1: Shows the X and Y center coordinates and the radii of the iris and pupil after processing the Daugman's operator on the 'histogram equalized' image.

7.2 Contrast enhancement

Contrast enhancement techniques are used to improve the quality of an image by making visible pixel details that are invisible in low contrast images. The distribution of pixel intensity values in a low contrast image are spread over a narrow range compared to the distribution of pixel intensity values in a high contrast image. One of the contrast enhancement techniques is given by the equation below [18]:

$$T_k(x, y) = a\,[f_k(x, y) - 127] + 127 \quad , \qquad (5)$$

where k denotes the number of pixel (1, 2, 3…) on which the transformation is applied,

(x, y) denote the x and y coordinates for a particular pixel on which the transformation is applied,

$f_k(x, y)$ denotes low contrast input image,

$T_k(x, y)$ denotes high contrast output image.

a > 1, for a increase in contrast and 0 <= a < 1, for a decreased contrast

Conditions to have a range of pixels intensity values from 0 to 255 (255 is maximum intensity value in the range (0 to 255) for grayscale images):

$$T_k(x, y) = \begin{cases} 0, & \text{if } T_k(x, y) < 0 \\ T_k(x, y), & \text{if } 0 <= T_k(x, y) < 255 \\ 255, & \text{if } T_k(x, y) > 255 \end{cases}$$

According to equation (5), the contrast of the input image is decreased or increased by multiplying every pixel value in the input image with a value a<1 or a>1 respectively. A graphic user interface (GUI) has been developed to demonstrate the dependence of the Daugman's operator performance from the input image quality. Figures 7-4 and 7-5 represent 5 images each. The top left image represents the input image. The top middle image represents the gray scale image of the input image to its left. The top right image represents the effect of change in contrast on the gray scaled image. The bottom right image represents the histogram of the contrast modified image. Finally, the bottom left image represents the result of the performance of Daugman's algorithm on the contrast modified image.

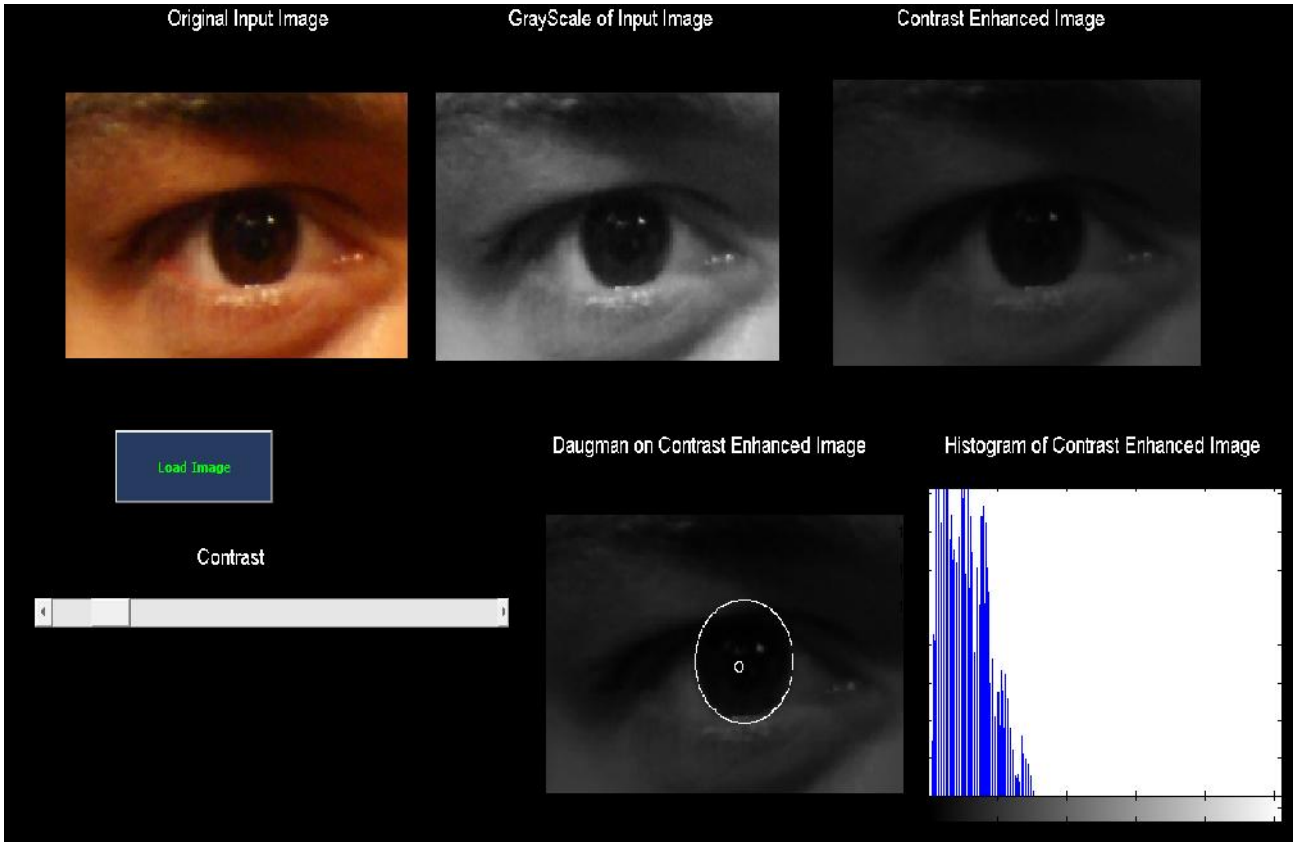

Figure 7-4: Shows the result of the performance of Daugman's algorithm on a low contrast image. The iris is detected correctly. However, due to very low contrast between the iris and the pupil, the pupil border with iris is wrongly detected.

As can be observed in Figure 7-4, Daugman's operator applied to a low contrast image has detected the iris outer border correctly, however has failed to detect the iris inner border. The pupil detection fails in the low contrast image since the difference in intensity values between the dark pupil and iris regions is too small (as shown in the histogram of the contrast modified image).

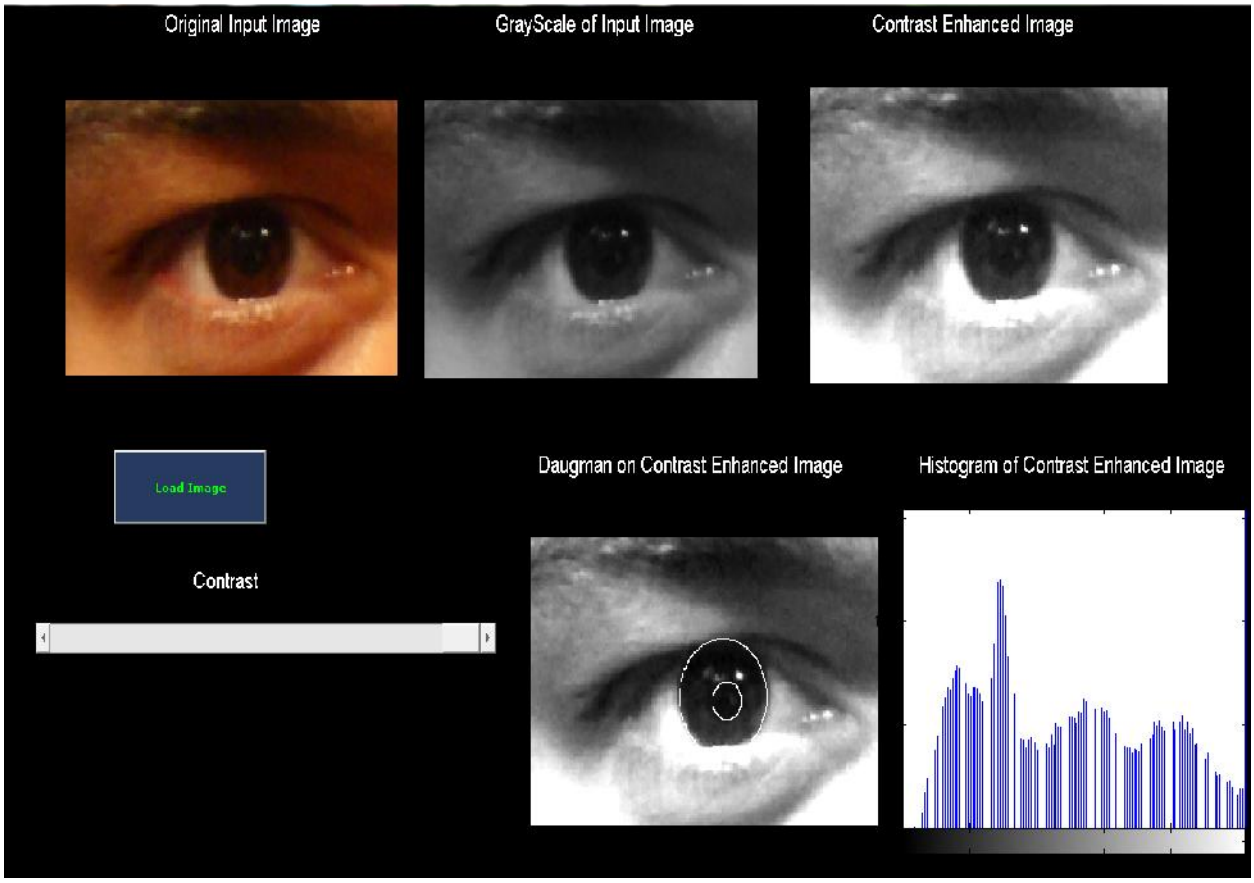

Figure 7-5: Shows the result of the performance of Daugman's algorithm on the same image with contrast enhanced. The iris is detected correctly. However due to a better contrast between the iris and the pupil, the pupil border with iris is also correctly detected.

After increasing the level of contrast for the same image, as shown in Figure 7-5 Daugman's operator detects both the iris and pupil borders correctly. In the contrast enhanced image of the same eye, the pixel intensity values are spread over a wider range of intensity values as represented by its histogram. A greater difference in intensity values between the circular pupil and the iris borders is observed.

Chapter 8

8 Effect of image noise on Daugman's integrodifferential operator performance

Though very effective, Daugman's operator not always segments the iris correctly when the input image of the iris contains noise in it. This noise can be in the form of reflection, or the eye in the image is not fully opened or the eyelashes covering some part of the iris area.

Low quality iris images result in poor recognition performance provided that traditional processing of iris images is applied [2]. As shown in iris images in Figures 8-1(a), 8-2 (a) and 8-3 (a) images having poor contrast, defocus blur, off angle iris, occlusion due to eyelashes etc have a negative impact on the iris detection process. Processing these images with the Daugman's algorithm failed to detect the iris outer and inner borders as shown in Figures 8-1(b), 8-2 (b) and 8-3(b).

To sum up, the segmentation of an iris using Daugman's integrodifferential operator may result in errors if the input image of the iris has one of the following effects [3]:

1. Poor focused iris images.
2. Off-angle iris images.
3. Rotated iris images.
4. Motion blurred iris images.
5. Iris obstructions due to eyelashes.
6. Iris obstructions due to eyelids.
7. Iris obstructions due to glasses.
8. Iris obstructions due to contact lenses.
9. Iris with specular reflections.
10. Iris with lighting reflections.
11. Partial captured iris images.
12. Out-of-iris images.

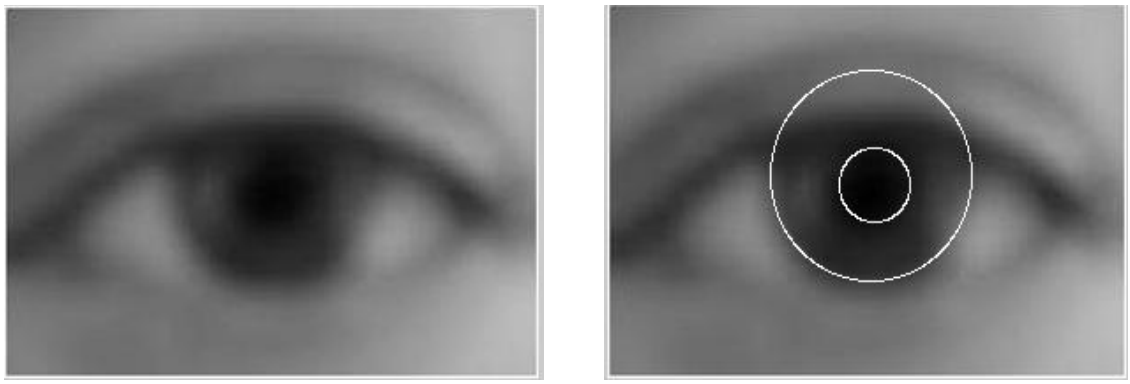

Figure 8-1: (a) Input blur image that does not have a sharp iris to sclera and iris to pupil contrast (b) iris and pupil detected incorrectly

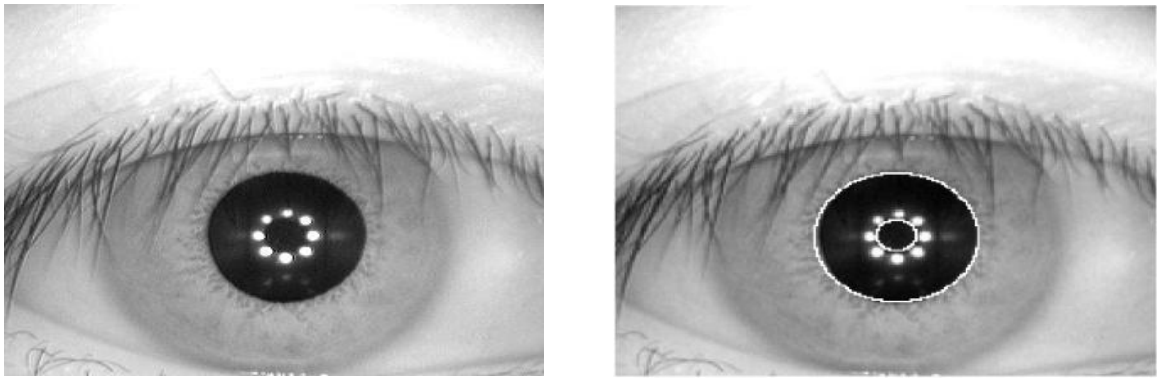

Figure 8-2: (a) Input noise image of light reflection (b) iris and pupil detected incorrectly

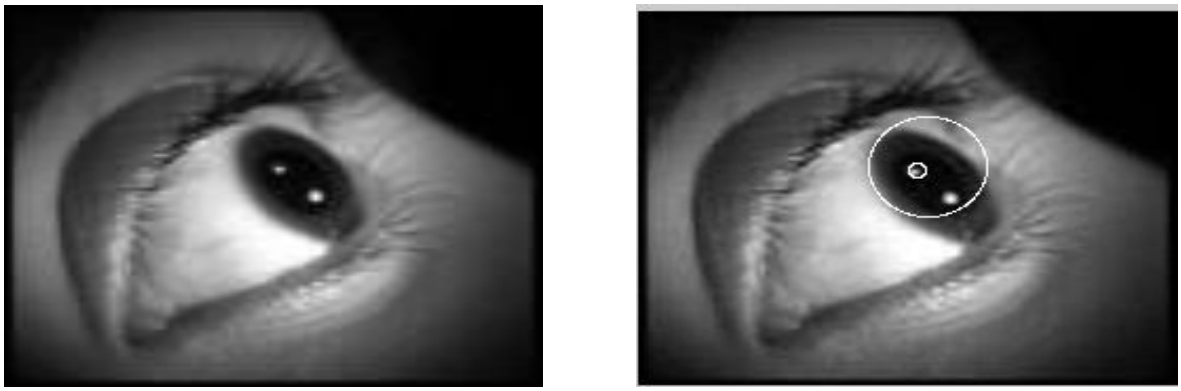

Figure 8-3: (a) Input noise image where the image of the is rotated at some angle (b) Iris and pupil incorrectly detected

9 Appendix A

9.1 Flow chart describing Daugman's method

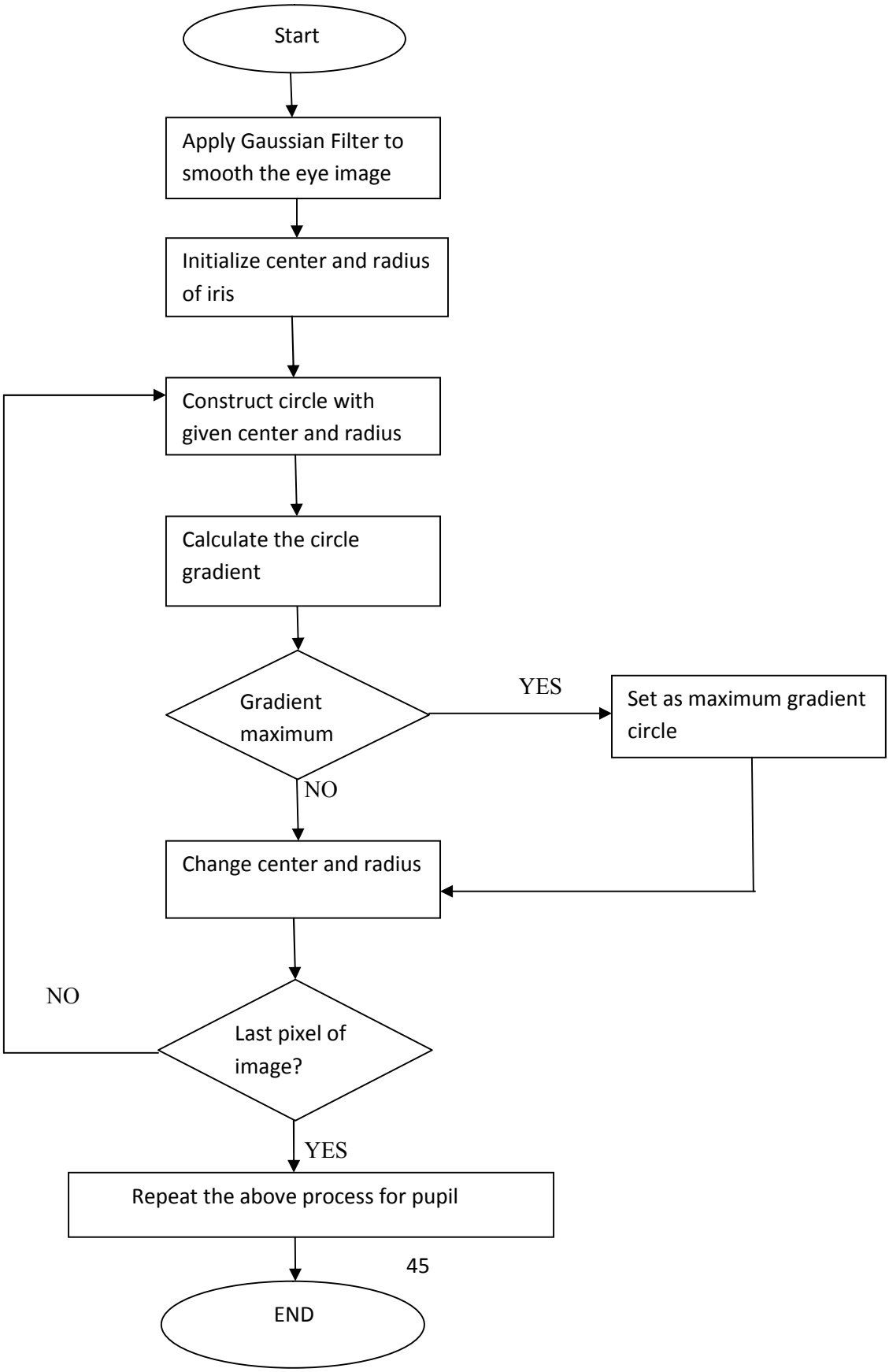

10 References

[1] Robert H Zakon . Hobbes' Internet Timeline. Significant dates in the history of the Internet. ©1993-2010

[2] Nathan D. Kalka, Jinyu Zuo, Natalia A. Schmid, Bojan Cukic Lane. Image quality assessment for iris. Department of Computer Science and Electrical Engineering, West Virginia University, Morgantown, WV 26506, USA

[3] Advances in biometric person authentication: 5th Chinese Conference on Biometric Recognition, SINOBIOMETRICS 2004, Guangzhou, China

[4] http://www.hrsid.com/iris-recognition

[5] John Daugman. Recognizing persons by their iris patterns. Cambridge University Cambridge, UK. 2001.

[6] L Dhir, N E Habib, D M Monro and S Rakshit. Effect of cataract surgery and pupil dilation on iris pattern recognition for personal authentication. 13 November 2009.

[7] J G Daugman. High confidence visual recognition of persons by a test of statistical independence. IEEE Trans. Pattern Anal.Mach. Intell, 15(11):1148–1160, 1993.

[8] R P Wildes. Iris recognition:an emerging biometric technology. Proc. IEEE, 85(9):1348–1363, 1997.

[9] Peihua Li, Xiaomin Liu. An incremental method for accurate iris segmentation. Int. Conf. on Pattern Recognition, Florida, USA, 2008.

[10] Gonzalez, Rafael C. & Woods, Richard E. (2002). Thresholding in digital image processing, pp. 595–611. Pearson Education. ISBN 81-7808-629-8

[11] Daugman J. "How iris recognition works." *IEEE Trans. CSVT,* vol. 14, no. 1. 2004.

[12] R.A. Haddad and A.N. Akansu. "A class of fast Gaussian binomial filters for speech and image processing," IEEE Transactions on Acoustics, Speech and Signal Processing, vol. 39

[13] Shapiro, L. G. & Stockman, G. C. "Computer Vision", page 137, 150. Prentence Hall, 2001

[14] Mark S. Nixon and Alberto S. Aguado. Feature extraction and image processing. Academic Press, 2008

[15] Bracewell, R. The Fourier transform and its applications (2nd ed.), McGraw–Hill, ISBN 0071160434 , 1986.

[16] J. Daugman. High confidence visual recognition of persons by a test of statistical independence. IEEE Transactions on Pattern Analysis and Machine Intelligence, Vol. 15, No. 11, 1993

[17] Rafael C. Gonzalez and Richard E. Woods. Digital Image Processing ISBN-10: 0201180758 | ISBN-13: 978-0201180756 | Publication Date: January 15, 2002 | Edition: 2nd

[18] http://image.ing.bth.se/ipl-bth/siamak.khatibi/AIPBTH11LP2/lectures/Lec-3.pdf